Original Article

Cinacalcet rectifies hypercalcemia in a patient with familial hypocalciuric hypercalcemia type 2 (FHH2) caused by a germline loss-of-function Gα11 mutation†

Caroline M. Gorvin[1], Fadil M. Hannan[1,2], Treena Cranston[3], Helena Valta[4], Outi Makitie[4,5], Camilla Schalin-Jantti[6], Rajesh V. Thakker[1]

[1] Academic Endocrine Unit, Radcliffe Department of Medicine, Oxford Centre for Diabetes, Endocrinology and Metabolism (OCDEM), University of Oxford, UK.
[2] Department of Musculoskeletal Biology, Institute of Ageing and Chronic Disease, University of Liverpool, UK.
[3] Oxford Molecular Genetics Laboratory, Churchill Hospital, Oxford, UK.
[4] Children's Hospital, University of Helsinki, Helsinki, Finland.
[5] Folkhälsan Research Center, Helsinki, Finland
[6] Division of Endocrinology, Abdominal Center, University of Helsinki and Helsinki University Hospital, Helsinki, Finland.

Address correspondence to: Camilla Schalin-Jantti at the Division of Endocrinology, Abdominal Center, Helsinki University Hospital, Finland (for clinical details), or Rajesh V. Thakker at the Academic Endocrine Unit, Oxford Centre for Diabetes, Endocrinology and Metabolism (OCDEM), Oxford, OX3 7LJ, UK. Tel no: 01865 857501. Fax no: 01865 875502. **Email:** camilla.schalin-jantti@hus.fi or rajesh.thakker@ndm.ox.ac.uk

†This article has been accepted for publication and undergone full peer review but has not been through the copyediting, typesetting, pagination and proofreading process, which may lead to differences between this version and the Version of Record. Please cite this article as doi: [10.1002/jbmr.3241]

Additional Supporting Information may be found in the online version of this article.

Initial Date Submitted June 30, 2017; Date Revision Submitted August 9, 2017; Date Final Disposition Set August 14, 2017

Journal of Bone and Mineral Research

DOI 10.1002/jbmr.3241

Abstract

G-protein subunit α-11 ($G\alpha_{11}$) couples the calcium-sensing receptor (CaSR) to phospholipase C (PLC)-mediated intracellular calcium (Ca^{2+}_i) and mitogen-activated protein kinase (MAPK) signaling, which in the parathyroid glands and kidneys regulates parathyroid hormone release and urinary calcium excretion, respectively. Heterozygous germline loss-of-function $G\alpha_{11}$ mutations cause familial hypocalciuric hypercalcemia type 2 (FHH2), for which effective therapies are currently not available. Here, we report a novel heterozygous $G\alpha_{11}$ germline mutation, Phe220Ser, which was associated with hypercalcemia in a family with FHH2. Homology modelling showed the wild-type Phe220 non-polar residue to form part of a cluster of hydrophobic residues within a highly conserved cleft region of $G\alpha_{11}$, which binds to and activates PLC; and predicted that substitution of Phe220 with the mutant Ser220 polar hydrophilic residue would disrupt PLC-mediated signalling. *In vitro* studies involving transient transfection of wild-type and mutant $G\alpha_{11}$ proteins into HEK293 cells, which express the CaSR, showed the mutant Ser220 $G\alpha_{11}$ protein to impair CaSR-mediated Ca^{2+}_i and extracellular signal-regulated kinase 1/2 (ERK) MAPK signaling, consistent with diminished activation of PLC. Furthermore, engineered mutagenesis studies demonstrated that loss of hydrophobicity within the $G\alpha_{11}$ cleft region also impaired signalling by PLC. The loss-of-function associated with the Ser220 $G\alpha_{11}$ mutant was rectified by treatment of cells with cinacalcet, which is a CaSR positive allosteric modulator. Furthermore, *in vivo* administration of cinacalcet to the proband harbouring the Phe220Ser $G\alpha_{11}$ mutation, normalised serum ionized calcium concentrations. Thus, our studies, which report a novel $G\alpha_{11}$ germline mutation (Phe220Ser) in a family with FHH2, reveal the importance of the $G\alpha_{11}$ hydrophobic cleft region for CaSR-mediated activation of PLC, and show that allosteric CaSR modulation can rectify the loss-of-function Phe220Ser mutation and ameliorate the hypercalcemia associated with FHH2.

Keywords: Parathyroid-related disorders; DISORDERS OF CALCIUM/PHOSPHATE METABOLISM; THERAPEUTICS; CELL/TISSUE SIGNALING- Endocrine Pathways

This article is protected by copyright. All rights reserved

Introduction

G-protein subunit alpha-11 ($G\alpha_{11}$) is a major downstream signalling partner of the cell-surface calcium-sensing receptor (CaSR), which is a family C G-protein coupled receptor (GPCR) that plays a pivotal role in the parathyroid and renal regulation of extracellular calcium (Ca^{2+}_e) concentrations[1]. $G\alpha_{11}$ belongs to the $G_{q/11}$ class of G-proteins that enhance phospholipase C (PLC) activity, thereby leading to formation of: inositol 1,4,5-trisphosphate (IP_3), which induces rapid increases in intracellular Ca^{2+} (Ca^{2+}_i) concentrations; and enhances diacylglycerol (DAG) formation, which in turn activates protein kinase C and the mitogen-activated protein kinase (MAPK) signalling cascade[2,3]. These signal transduction events allow the CaSR to respond to small fluctuations in the prevailing Ca^{2+}_e concentrations ($[Ca^{2+}]_e$) and to induce alterations in parathyroid hormone (PTH) secretion and urinary calcium excretion[4].

The identification of germline heterozygous mutations of $G\alpha_{11}$, which is encoded by the *GNA11* gene on chromosome 19p13.3, that result in familial hypocalciuric hypercalcemia (FHH) has demonstrated the importance of this G-protein subunit in Ca^{2+}_e homeostasis[5]. FHH is an autosomal dominant disorder characterized by lifelong elevations of serum calcium concentrations in association with normal or mildly raised serum PTH concentrations and low urinary calcium excretion (calcium-to-creatinine clearance ratio <0.01)[4]. FHH comprises three genetically distinct conditions, designated as FHH types 1-3. FHH1 (OMIM #145980) is caused by loss-of-function CaSR mutations[1]. FHH2 (OMIM #145981) is caused by loss-of-function $G\alpha_{11}$ mutations; to date, three FHH2-associated mutations have been reported, comprising two missense mutations, Thr54Met and Leu135Gln, and an in-frame isoleucine deletion at codon 200 (Ile200del)[5,6] (Supplemental Figure 1). FHH3 (OMIM #600740) is caused by loss-of-function mutations of the adaptor protein-2 sigma-1 (*AP2S1*) gene, encoding AP2σ, which is involved in the clathrin-mediated endocytosis of GPCRs, such as the CaSR[1].

Positive allosteric modulators of the CaSR, known as calcimimetics, represent a targeted therapy for patients with symptomatic FHH. Indeed, cinacalcet, a licenced calcimimetic drug, has been used to ameliorate symptomatic hypercalcemia in patients with FHH1 and FHH3[7-9]. However, such effects of cinacalcet in FHH2 patients have not been reported, although cinacalcet has been shown *in vitro*, to rectify signaling abnormalities associated with FHH2-causing $G\alpha_{11}$ mutations[10]. Here, we report the effectiveness of cinacalcet in ameliorating the signalling defects and hypercalcemia due to a previously unreported FHH2-associated $G\alpha_{11}$ mutation, Phe220Ser.

Materials and Methods

Case Report

The proband (individual II.1, Figure 1A) was a 33 year old male who presented with headaches, constipation and pruritus. Biochemical investigations revealed hypercalcemia, hypophosphatemia, raised plasma PTH concentrations, and a low calcium-to-creatinine clearance ratio (Table 1). A DXA scan showed normal bone mineral density values at the spine and hip (Table 1). A skin biopsy, undertaken to investigate the pruritus, demonstrated folliculitis (Table 1). His father, and three of his four children, also had hypercalcemia, constipation and/or headaches (Table 1). Two of his affected children had eczema, and the proband's father had sustained an osteoporotic vertebral fracture. The familial hypercalcemia and reduced urinary calcium excretion were consistent with FHH, however *CASR* or *AP2S1* mutations were not identified. Informed consent was obtained from individuals and where appropriate, parents and guardians of children, using protocols approved by the Research Ethics Committee of the Helsinki University Hospital.

Mutational Analysis

DNA sequence analyses of *GNA11* exons 1-7 and adjacent splice sites (NM_002067) was performed using leucocyte DNA and gene-specific primers (SigmaAldrich), as previously reported[5,6]. Polymorphic variants were identified from public databases (Supplemental Table 1).

Protein Sequence Alignment and Three-Dimensional Modeling of $G\alpha_{11}$ Structure

Protein sequences of $G\alpha_{11}$ orthologs were aligned using ClustalOmega (http://www.ebi.ac.uk/Tools/msa/clustalo/)[6]. $G\alpha_{11}$ three-dimensional modeling was undertaken using the reported three-dimensional structures of: $G\alpha_q$ in complex with phospholipase C-β3 (Protein Data Bank accession no. 3OHM)[11]; $G\alpha_q$ in complex with the

small molecule inhibitor YM-254890 (Protein Data Bank accession no. 3AH8)[12]; and $G\alpha_q$ in complex with the regulator of G-protein signaling 2 (RGS2) (Protein Data Bank accession no. 4EKC and 4QJ3)[13,14]. The $G\alpha_q$ protein, which shares 90% identity at the amino acid level with $G\alpha_{11}$, was used because crystal structures of $G\alpha_{11}$ are not available. Figures were prepared using the PyMOL Molecular Graphics System, Schrodinger.

Cell culture and Transfection

Mutations were introduced into the previously described pBI-CMV2-*GNA11* expression construct by site-directed mutagenesis using the Quikchange Lightning Kit (Agilent Technologies) and gene-specific primers (SigmaAldrich). Wild-type or mutant pBI-CMV2-*GNA11* constructs were transiently transfected into HEK293 cells stably expressing CaSR (HEK293-CaSR) using Lipofectamine 2000 (LifeTechnologies), as described[15,16]. The pBI-CMV2-*GNA11* bidirectional vector allows for co-expression of $G\alpha_{11}$ and GFP at equivalent levels[5]. HEK293-CaSR cells were maintained in DMEM-Glutamax media (Gibco) that has a calcium concentration of 1.80 mM. The presence of mutations was verified using dideoxynucleotide sequencing with the BigDye Terminator v3.1 Cycle Sequencing Kit (Life Technologies) and an automated detection system (ABI3730 Automated capillary sequencer; Applied Biosystems)[17]. Luciferase reporter constructs (pGL4.30-NFAT, pGL4.33-SRE) were purchased from Promega. HEK293 cells were used because suitable parathyroid and renal tubular cells are not available, and HEK293 cells have been established as a model for the functional expression of $G\alpha_{11}$ proteins[5,15,16]. HEK-CaSR cells were cultured in high-glucose DMEM (Invitrogen) supplemented with 10% fetal bovine serum and 1% geneticin at 37°C, 5% CO_2[5]. Successful transfection was confirmed by visualising GFP fluorescence using an Eclipse E400 fluorescence microscope with an epifluorescence filter, and images were captured using a DXM1200C digital camera and NIS Elements software (Nikon)[5,16]. The

expression of $G\alpha_{11}$ and CaSR proteins was confirmed by Western blot analyses using $G\alpha_{11}$ (Santa Cruz Biotechnologies), anti-calnexin (Millipore) or anti-CaSR (Abcam) antibodies. Calnexin, a housekeeping protein, was used as a loading control. The Western blots were visualised using an Immuno-Star Western C kit (BioRad) on a BioRad Chemidoc XRS+ system[6].

Fluo-4 intracellular calcium assay

Ca^{2+}_e-induced Ca^{2+}_i responses were measured by Fluo-4 calcium assays adapted from methods previously published[18]. HEK-CaSR cells were plated in poly-L-lysine treated black-walled 96-well plates (Corning), and transiently transfected with 1000ng/ml pBI-CMV2-*GNA11*. Cells were conditioned in serum-free media (1.8 mM Ca^{2+}_e) overnight, then incubated in Ca^{2+}- and Mg^{2+}-free Hanks Balanced Salt Solution (HBSS) for 1 hour, followed by loading with Fluo-4 dye, prepared according to manufacturer's instructions (Invitrogen). Cells were loaded for 40 minutes at 37°C, then either: a 20% aqueous solution of 2-hydoxypropyl-β-cyclodextrin (vehicle); or 30 or 100 nM cinacalcet was added. Cells were then incubated for a further 20 minutes at 37°C[18]. Baseline measurements were made and $CaCl_2$ was injected into each well to increase the $[Ca^{2+}]_e$ in a stepwise manner from 0.5-10mM $[Ca^{2+}]_e$, using an automated system. Changes in Ca^{2+}_i were recorded on a PHERAstar instrument (BMG Labtech) at 37°C with an excitation filter of 485nm and an emission filter of 520nm. The peak mean fluorescence ratio of the transient response after each individual stimulus was measured using MARS data analysis software (BMG Labtech), and expressed as a normalized response. Nonlinear regression of concentration-response curves was performed with GraphPad Prism using the normalized response at each $[Ca^{2+}]_e$ for each separate experiment for the determination of the EC_{50} (i.e. $[Ca^{2+}]_e$ required for 50% of the maximal response). Assays were performed in 4-12

biological replicates for each of the expression constructs. Statistical analysis was performed using the *F*-test[5,6].

Luciferase reporter assay

HEK-CaSR cells were seeded in 48-well plates and transiently transfected with 100ng/mL pBI-CMV2-*GNA11* wild-type (WT) or mutant proteins, 100ng/ml luciferase construct (either pGL4-NFAT or pGL4-SRE) and 10ng/ml pRL control vector for 48 hours. Cells were incubated in serum-free media for 12 hours, followed by treatment of cells for 4 hours with 0.1-10mM $CaCl_2$. Cells were lysed and assays performed with Dual-Glo luciferase (Promega) on a Veritas Luminometer (Promega), as previously described[19]. Luciferase:renilla ratios were expressed as fold-changes relative to responses at basal $CaCl_2$ concentrations. For studies with cinacalcet (Cambridge Bioscience), the drug was added to cells, as described previously[10,19]. All assays were performed using 4 biological replicates on up to 3 independent occasions. Statistical analysis was performed by 2-way ANOVA with Tukey's multiple-comparisons test using GraphPad Prism 6.

Measurement of ERK phosphorylation

HEK-CaSR cells were seeded in 48-well plates and transfected with 200ng/mL WT or mutant $G\alpha_{11}$, 48-hours prior to performance of assays. Transfected cells were incubated in serum-free media 12 hours prior to treatment of cells with 0.1-10mM $CaCl_2$. Cells were then lysed in Surefire lysis buffer, and AlphaScreen Surefire ERK assays measuring phosphorylated and total proteins were performed, as previously described[10,19]. The fluorescence signal in both assays was measured using the PHERAstar FS microplate reader (BMG Labtech)[19]. The ratio of phosphorylated ERK to total ERK measured at each $[Ca^{2+}]_o$ were normalized to the mean

responses of WT expressing cells and expressed as a fold-change of responses obtained at basal (0.1 mM) $[Ca^{2+}]_e$. All assay conditions were performed in 4 biological replicates on up to 4 independent occasions. Statistical analysis was performed by 2-way ANOVA with Tukey's multiple-comparisons test using GraphPad Prism 6.

Web Resources

Predicted effect of the mutation was assessed using Polyphen-2 (http://genetics.bwh.harvard.edu/pph2/)[20] and MutationTasting (http://www.mutationtaster.org/)[21].

Statistics

All studies involved between 4-16 separate transfection experiments. Statistical analyses for $Ca^{2+}{}_i$ EC_{50} used the *F*-test[19], and two-way ANOVA with Tukey's multiple-comparisons test was used for pERK and luciferase reporter assays. Analyses were undertaken using GraphPad Prism, and a value of $p<0.05$ was considered significant.

Results

Identification of a novel Phe220Ser $G\alpha_{11}$ mutation in a family with FHH2

DNA sequence analysis of *GNA11* in the proband identified a heterozygous T-to-C transition at nucleotide c.659 (Figure 1A), resulting in a missense substitution of the WT Phe to a mutant Ser at residue 220 of the $G\alpha_{11}$ protein. Bioinformatic analyses predicted the Phe220Ser variant to be damaging and likely disease-causing (Polyphen-2 score = 1, MutationTasting score = 0.99). The absence of this DNA sequence abnormality in >67,200 exomes from the NHLBI-ESP and Exome Aggregation Consortium cohorts, together with evolutionary conservation of the Phe220 residue in $G\alpha_{11}$ orthologs and Gα-subunit paralogs (Figure 1B), also indicated that the Phe220Ser abnormality likely represents a pathogenic mutation rather than a benign polymorphic variant.

The Phe220Ser mutation is located in the switch II region of $G\alpha_{11}$ and predicted to impair PLC activation

Homology modelling, using crystal structures of the related $G\alpha_q$ protein[11,12,22], revealed the WT Phe220 residue to be located within the α2-helix of the flexible switch II region of the $G\alpha_{11}$ GTPase domain (Figure 1B-C, Supplemental Figure 1), and to comprise part of a hydrophobic cluster of amino acids located within a cleft region formed by switch II and the adjacent α3-helix that interact with PLC upon G-protein activation (Figure 1C-D)[11]. Substitution of the non-polar hydrophobic WT Phe220 residue, with the mutant polar hydrophilic Ser220 residue is predicted to disrupt $G\alpha_{11}$ function by impairing PLC activation and signaling.

The Gα11 Phe220Ser mutation impairs Ca^{2+}_i responses

The Phe220Ser mutation is predicted to diminish PLC activation, and we therefore assessed its effects on Ca^{2+}_i mobilization, which has previously been shown to be enhanced downstream of PLC by the $G_{q/11}$ proteins[23-26]. HEK293 cells stably expressing the CaSR (HEK-CaSR) were transiently transfected with pBI-CMV2-*GNA11* constructs expressing the WT (Phe220) or mutant (Ser220) Gα11 proteins (Supplemental Figure 2). The Ca^{2+}_i responses of the mutant Ser220 Gα11-expressing HEK-CaSR cells, revealed that a significantly greater $[Ca^{2+}]_e$ was required to achieve half-maximal (EC_{50}) Ca^{2+}_i responses, when compared with WT-expressing cells (Figure 2A). Thus, the Ser220 mutant-expressing cells showed a rightward shift in the concentration-response curve, with a significantly elevated mean EC_{50} value ($p<0.001$) of 2.93 mM (95% confidence interval (CI), 2.80-3.07 mM), compared with 2.40 mM (95% CI, 2.27-2.53 mM) for WT expressing cells. The Ca^{2+}_i responses were also assessed by measurement of nuclear factor of activated T-cells (NFAT), which is a downstream mediator of Ca^{2+}_i signalling[27]. NFAT fold-change responses were determined using a luciferase reporter assay, and these studies showed that HEK-CaSR cells expressing the Ser220 Gα11 mutant had a significantly reduced fold-change response (fold-change = 2.3±0.3) following exposure to 5mM $[Ca^{2+}]_e$, when compared with WT cells (fold-change = 4.8±0.4, $p<0.001$) (Figure 2B). These data demonstrated that the Gα11 Phe220Ser mutation impairs CaSR-mediated Ca^{2+}_i responses, consistent with a loss-of-function associated with FHH2.

The Gα11 Phe220Ser mutation impairs ERK phosphorylation

The ERK protein represents a major component of the MAPK signaling cascade, which has previously been demonstrated to be activated by PLC [3,28]. We assessed the effect of the Gα11 Phe220Ser mutation on ERK phosphorylation by measuring phosphorylated ERK (pERK) in response to increases in Ca^{2+}_e in WT and mutant Ser220 Gα11 expressing cells using the AlphaScreen assay, and also by assessing serum-response element (SRE)-mediated

transcriptional activity, which is regulated by ERK signalling[19]. The pERK responses of the Ser220 $G\alpha_{11}$ mutant were shown to be significantly reduced. Thus, the Ser220 $G\alpha_{11}$ mutant led to significant reductions in: pERK-to-total ERK ratios (Ser220 response at 5mM Ca^{2+}_e = 3.7±0.4 versus Phe220 = 6.1±0.3, $p<0.0001$) (Figure 2C); and to SRE reporter fold-changes (Ser220 fold-change at 5mM Ca^{2+}_e = 6.5±0.5 versus Phe220 fold-change = 11.8±0.7, $p<0.0001$) (Figure 2D). Thus, the $G\alpha_{11}$ Phe220Ser mutation impaired CaSR-mediated ERK phosphorylation.

Phe220 forms part of a hydrophobic cluster of $G\alpha_{11}$ residues required for PLC-mediated signalling

To further determine the mechanistic role of the Phe220 residue and the importance of residue 220 hydrophobicity for $G\alpha_{11}$ function and PLC-mediated signalling (Figure 1C), we engineered mutations of Phe220 to Leu and Ala, which are hydrophobic residues, and to Arg and Glu, which are hydrophilic positively- and negatively-charged residues, respectively, and studied their effect on Ca^{2+}_i and ERK responses following transient expression in HEK-CaSR cells (Figure 3). The Leu220 and Ala220 $G\alpha_{11}$ mutants did not alter Ca^{2+}_i responses (Figure 3A-B, Supplemental Figure 3), or ERK activity, as measured using the pERK AlphaScreen and SRE reporter assays (Figure 3C-D). In contrast, the positively-charged Arg220, and negatively-charged Glu220 $G\alpha_{11}$ mutants, respectively, enhanced and impaired Ca^{2+}_i and ERK signalling responses in HEK-CaSR cells (Figure 3, Supplemental Figure 3). Thus, these findings demonstrated that a hydrophobic residue at position 220 is required for signalling via PLC. The enhancement of CaSR-mediated signaling by the Arg220 $G\alpha_{11}$ mutant may be explained by its structural effect on the G_{11} heterotrimer. Homology modelling, using crystal structures of the related G_q protein in complex with $G\beta\gamma$[12] revealed that the Arg220 residue faces away from the hydrophobic cluster, into the region at which $G\alpha$ and $G\beta\gamma$ bind, a hydrophobic region that

is necessary for Gα activation[29] (Supplemental Figure 4). Disruption of this hydrophobic region has previously been shown to cause constitutive activation[29], and modelling predicts that the Arg220 residue, which is charged and hydrophilic, disrupts this region, thus enhancing activation by impairing Gαβγ association (Supplemental Figure 4). To investigate the importance of the $G\alpha_{11}$ hydrophobic cleft, formed by switch II and the α3-helix (Figure 1C-D), for PLC activation, we engineered mutations of three other hydrophobic residues, Ile217, Val223 and Trp263, within this region, to either an Ala residue, to retain hydrophobicity, or to a Glu residue, to lose hydrophobicity, and studied the effects of these mutants on Ca^{2+}_i and ERK responses following their transient expression in HEK-CaSR cells (Supplemental Figure 5). This demonstrated that substitution to Ala of only one hydrophobic residue, Ile217, altered PLC-mediated signaling (Figure 4A-C, Supplemental Figure 6). In contrast, substitution of any of the Ile217, Val223 and Trp263 hydrophobic residues to a Glu residue led to a significant reduction in Ca^{2+}_i and ERK responses (Figure 4D-F, Supplemental Figure 6). Thus, hydrophobicity of the switch II-α3 cleft is important for PLC activation.

Cinacalcet rectifies the impaired PLC signalling responses and hypercalcemia caused by the Phe220Ser $G\alpha_{11}$ mutation

To determine whether cinacalcet may be an effective therapy for FHH2, we evaluated the effects of different cinacalcet concentrations (0, 30 and 100nM) on the altered PLC signaling responses due to the Phe220Ser $G\alpha_{11}$ mutant. Treatment of mutant Ser220 $G\alpha_{11}$-expressing HEK-CaSR cells with 30nM cinacalcet, failed to normalize the impaired Ca^{2+}_i and SRE reporter responses (Figure 5A-C); however, 100 nM cinacalcet, reduced the EC_{50} values, and increased NFAT and SRE reporter activity (Figure 5A-C), such that these values were not significantly different from untreated WT cells. These *in vitro* findings suggested that higher doses of cinacalcet may be required for the treatment of patients harboring the Phe220Ser $G\alpha_{11}$

mutation. Cinacalcet was administered to the FHH2 proband as he had symptoms such as headaches, constipation and pruritus (Table 1), which may have been caused by the hypercalcemia. The proband was initially commenced on 30 mg/day of oral cinacalcet for 3 months, and in keeping with the above cellular studies, which showed a lack of efficacy when using low cinacalcet concentrations, the 30mg/day dose failed to normalize his elevated serum calcium concentrations (Figure 5D). However, increasing the dose of cinacalcet to 60 mg/day, successfully lowered the serum concentrations of: ionized calcium from 1.42 to 1.26 mmol/L (normal range 1.16-1.30 mmol/L) (Figure 5D); and PTH from 98 to 58 ng/L (normal range 8-73 ng/L). Although the proband became normocalcemic on cinacalcet, the pruritus, from which he suffered the most, did not resolve, and cinacalcet 60 mg/day was discontinued after 4 months. His hypercalcemia returned upon cessation of cinacalcet therapy (Figure 5D).

Discussion

Our studies have identified a previously unreported FHH2-causing heterozygous $G\alpha_{11}$ germline loss-of-function mutation that represents the first loss-of-function $G\alpha_{11}$ mutation to be located within the Gα-subunit switch regions. The switch regions are comprised of three flexible peptide loops, which are highly conserved amongst all classes of Gα-subunits, and undergo substantial conformational changes depending on the guanine nucleotide-bound state of the Gα subunit[30]. In the GTP-bound state, these peptide loops switch their conformation to one that facilitates coupling with downstream effector proteins[31]. The Phe220Ser mutation is located in the switch II region, which is predicted to bind and activate PLC[11], and our in vitro assessment of Ca^{2+}_i and pERK responses in cells expressing the mutant Ser220 $G\alpha_{11}$ demonstrated an impairment of signalling that is, at least in part, mediated by PLC[26,32]. Furthermore, our mutagenesis studies showed that Phe220 forms part of a group of hydrophobic residues that are required for coupling to PLC, and that Phe220 is located in a key region within this hydrophobic cleft, such that substitution of the hydrophobic Phe220 residue for a hydrophilic positively (Arg) or negatively (Glu) charged residue resulted, respectively, in a gain- or loss-of $G\alpha_{11}$ function, thereby indicating that mutations of Phe220 can either retard or enhance the switch II conformational changes that occur upon G-protein activation.

These studies have involved a comprehensive investigation of the effect of FHH2-associated $G\alpha_{11}$ mutations on PLC signalling at both the cytosolic (i.e. Ca^{2+}_i and pERK) and transcriptional (i.e. NFAT and SRE reporter) level, and demonstrate that all readouts are affected by FHH2 mutations. The need to measure several signal outputs is increasingly important as recent studies have shown that GPCRs can couple to multiple G-proteins to enhance their signaling capabilities and respond in diverse tissues[33,34]. Indeed, this is particularly the case in $G\alpha_{11}$ mutant cells, where it has been hypothesised that other G-proteins,

in particular $G\alpha_q$, may compensate for some of the functions of $G\alpha_{11}$ giving rise to the milder phenotype observed in FHH2[5,6]. Our studies of the transcriptional events downstream of CaSR activation indicate that Ca^{2+}_i signaling is more severely impaired than ERK signalling, as the Ser220 $G\alpha_{11}$ mutant cells have more robust SRE signals than NFAT signals. MAPK signalling is known to occur downstream of several G-proteins and can be used as a surrogate to assess multiple G-protein families[32,35]. The differences observed in Ca^{2+}_i signaling compared to ERK signaling in $G\alpha_{11}$ Ser220 mutant cells indicates that $G\alpha_{11}$ may preferentially signal via Ca^{2+}_i, or that other G-proteins are able to compensate for a reduction in $G\alpha_{11}$-mediated ERK responses in FHH2 mutant cells.

The $G\alpha_{11}$ protein is considered to be ubiquitously expressed[36], thus raising the possibility that germline $G\alpha_{11}$ mutations may be associated with non-calcitropic phenotypes. Indeed, in addition to constipation most of the affected family members had folliculitis or eczematous skin lesions, which may potentially represent a non-calcitropic phenotype of FHH2. This is plausible as somatic activating $G\alpha_{11}$ mutations have been reported to cause cutaneous pigmentatory disorders such as dermal melanocytosis [37], and studies of atopic dermatitis, which is characterised by impaired epithelial barrier function and eczematous skin lesions, have revealed that $G_{q/11}$-coupled chemokine receptors facilitate the migration of inflammatory cells within the dermis [38]. However, such roles of loss-of-function $G\alpha_{11}$ mutations in cutaneous disorders remain to be elucidated, and these may be facilitated by studies of additional FHH2 patients and appropriate mouse models.

Our studies have also demonstrated that cinacalcet-mediated allosteric modulation of the CaSR successfully rectified the loss-of-function associated with the Phe220Ser $G\alpha_{11}$ mutation *in vitro* and *in vivo*. However, a higher concentration of cinacalcet was required to normalise the

signalling responses of cells expressing the $G\alpha_{11}$ mutant Ser220, when compared to other FHH2-causing $G\alpha_{11}$ mutants[10]. These *in vitro* findings suggest that loss-of-function mutations located within the $G\alpha_{11}$ switch regions may alter the efficacy of calcimimetic compounds, and it is notable that the hypercalcemic proband with a Phe220Ser $G\alpha_{11}$ mutation required an increase in the dose of cinacalcet from 30 to 60 mg daily to normalize the elevated serum calcium concentrations (Figure 2C). Moreover, cinacalcet in the patient exerted an inhibitory effect on PTH secretion, as observed by a normalization of serum PTH concentrations. Cinacalcet may be rectifying the impaired signaling by the mutant Phe220Ser $G\alpha_{11}$ by increasing signaling through the WT $G\alpha_{11}$, which is present endogenously in HEK293 cells and the cells of the heterozygous patient, and/or compensatory signaling by the closely-related $G\alpha_q$, which activates the same signaling pathways downstream of CaSR. Importantly, hypocalcemia or adverse effects such as nausea and vomiting, which may affect >25% of patients[39], were not observed in the patient, despite receiving a higher dose of cinacalcet.

In conclusion, we have identified a FHH2-causing mutation, which affects the $G\alpha_{11}$ switch region and disrupts PLC-mediated signaling, and have also shown that cinacalcet can rectify these signaling disturbances and be used successfully to treat the hypercalcemia caused by this germline loss-of-function $G\alpha_{11}$ mutation.

Acknowledgements

This work was supported by: Academy of Finland, Sigrid Jusélius Foundation and Folkhälsan Research Foundation (to OM); Finska Lakaresallskapet and Helsinki University Hospital Research Funds (to CS-J); a Wellcome Trust Senior Investigator Award (to RVT); National Institute for Health Research (NIHR) Oxford Biomedical Research Centre Program (to RVT); and NIHR Senior Investigator Award (to RVT).

Author Roles

CMG, FMH, CS-J and RVT conceived and coordinated the study; HV, OM and CS-J provided the clinical data; CS-J performed the cinacalcet trial in the proband. CMG and TC performed and analyzed the experiments; CMG, FMH, CS-J and RVT wrote the manuscript; and all authors reviewed the results and approved the final version of the manuscript.

Disclosure: F.M.H and R.V.T. have received grant funding from NPS/Shire Pharmaceuticals and GlaxoSmithKline for unrelated studies involving the use of calcium-sensing receptor allosteric inhibitors. R.V.T. has also received grants from Novartis Pharma AG and the Marshall Smith Syndrome Foundation for unrelated studies.

References

1. Hannan FM, Babinsky VN, Thakker RV. Disorders of the calcium-sensing receptor and partner proteins: insights into the molecular basis of calcium homeostasis. Journal of molecular endocrinology. Oct 2016;57(3):R127-42.
2. Hofer AM, Brown EM. Extracellular calcium sensing and signalling. Nature reviews Molecular cell biology. Jul 2003;4(7):530-8.
3. Wu DQ, Lee CH, Rhee SG, Simon MI. Activation of phospholipase C by the alpha subunits of the Gq and G11 proteins in transfected Cos-7 cells. The Journal of biological chemistry. Jan 25 1992;267(3):1811-7.
4. Hannan FM, Thakker RV. Calcium-sensing receptor (CaSR) mutations and disorders of calcium, electrolyte and water metabolism. Best practice & research Clinical endocrinology & metabolism. Jun 2013;27(3):359-71.
5. Nesbit MA, Hannan FM, Howles SA, Babinsky VN, Head RA, Cranston T, et al. Mutations affecting G-protein subunit alpha11 in hypercalcemia and hypocalcemia. The New England journal of medicine. Jun 27 2013;368(26):2476-86.
6. Gorvin CM, Cranston T, Hannan FM, Rust N, Qureshi A, Nesbit MA, et al. A G-protein Subunit-alpha11 Loss-of-Function Mutation, Thr54Met, Causes Familial Hypocalciuric Hypercalcemia Type 2 (FHH2). Journal of bone and mineral research : the official journal of the American Society for Bone and Mineral Research. Jun 2016;31(6):1200-6.
7. Howles SA, Hannan FM, Babinsky VN, Rogers A, Gorvin CM, Rust N, et al. Cinacalcet for Symptomatic Hypercalcemia Caused by AP2S1 Mutations. The New England journal of medicine. Apr 7 2016;374(14):1396-8.
8. Festen-Spanjer B, Haring CM, Koster JB, Mudde AH. Correction of hypercalcaemia by cinacalcet in familial hypocalciuric hypercalcaemia. Clinical endocrinology. Feb 2008;68(2):324-5.
9. Tenhola S, Hendy GN, Valta H, Canaff L, Lee BS, Wong BY, et al. Cinacalcet Treatment in an Adolescent With Concurrent 22q11.2 Deletion Syndrome and Familial Hypocalciuric Hypercalcemia Type 3 Caused by AP2S1 Mutation. The Journal of clinical endocrinology and metabolism. Jul 2015;100(7):2515-8.
10. Babinsky VN, Hannan FM, Gorvin CM, Howles SA, Nesbit MA, Rust N, et al. Allosteric Modulation of the Calcium-sensing Receptor Rectifies Signaling Abnormalities Associated with G-protein alpha-11 Mutations Causing Hypercalcemic and Hypocalcemic Disorders. The Journal of biological chemistry. May 13 2016;291(20):10876-85.
11. Waldo GL, Ricks TK, Hicks SN, Cheever ML, Kawano T, Tsuboi K, et al. Kinetic scaffolding mediated by a phospholipase C-beta and Gq signaling complex. Science. Nov 12 2010;330(6006):974-80.
12. Nishimura A, Kitano K, Takasaki J, Taniguchi M, Mizuno N, Tago K, et al. Structural basis for the specific inhibition of heterotrimeric Gq protein by a small molecule. Proceedings of the National Academy of Sciences of the United States of America. Aug 03 2010;107(31):13666-71.
13. Nance MR, Kreutz B, Tesmer VM, Sterne-Marr R, Kozasa T, Tesmer JJG. Structural and Functional Analysis of the Regulator of G Protein Signaling 2-G alpha(q) Complex. Structure. Mar 5 2013;21(3):438-48.
14. Lyon AM, Begley JA, Manett TD, Tesmer JJ. Molecular mechanisms of phospholipase C beta3 autoinhibition. Structure. Dec 02 2014;22(12):1844-54.

15. Nesbit MA, Hannan FM, Howles SA, Reed AA, Cranston T, Thakker CE, et al. Mutations in AP2S1 cause familial hypocalciuric hypercalcemia type 3. Nature genetics. Research Support, Non-U.S. Gov't Jan 2013;45(1):93-7. Epub 2012/12/12.
16. Hannan FM, Howles SA, Rogers A, Cranston T, Gorvin CM, Babinsky VN, et al. Adaptor protein-2 sigma subunit mutations causing familial hypocalciuric hypercalcaemia type 3 (FHH3) demonstrate genotype-phenotype correlations, codon bias and dominant-negative effects. Human molecular genetics. Sep 15 2015;24(18):5079-92.
17. Newey PJ, Gorvin CM, Cleland SJ, Willberg CB, Bridge M, Azharuddin M, et al. Mutant prolactin receptor and familial hyperprolactinemia. The New England journal of medicine. Case Reports. Nov 21 2013;369(21):2012-20. Epub 2013/11/08.
18. Leach K, Gregory KJ, Kufareva I, Khajehali E, Cook AE, Abagyan R, et al. Towards a structural understanding of allosteric drugs at the human calcium-sensing receptor. Cell research. May 2016;26(5):574-92.
19. Gorvin CM, Hannan FM, Howles SA, Babinsky VN, Piret SE, Rogers A, et al. Galpha11 mutation in mice causes hypocalcemia rectifiable by calcilytic therapy. JCI insight. Feb 09 2017;2(3):e91103.
20. Adzhubei I, Jordan DM, Sunyaev SR. Predicting functional effect of human missense mutations using PolyPhen-2. Current protocols in human genetics / editorial board, Jonathan L Haines [et al]. Jan 2013;Chapter 7:Unit7 20.
21. Schwarz JM, Cooper DN, Schuelke M, Seelow D. MutationTaster2: mutation prediction for the deep-sequencing age. Nature methods. Apr 2014;11(4):361-2.
22. Tesmer VM, Kawano T, Shankaranarayanan A, Kozasa T, Tesmer JJ. Snapshot of activated G proteins at the membrane: the Galphaq-GRK2-Gbetagamma complex. Science. Dec 09 2005;310(5754):1686-90.
23. Bai M, Trivedi S, Lane CR, Yang Y, Quinn SJ, Brown EM. Protein kinase C phosphorylation of threonine at position 888 in Ca2+o-sensing receptor (CaR) inhibits coupling to Ca2+ store release. The Journal of biological chemistry. Aug 14 1998;273(33):21267-75. Epub 1998/08/08.
24. Brown E, Enyedi P, LeBoff M, Rotberg J, Preston J, Chen C. High extracellular Ca2+ and Mg2+ stimulate accumulation of inositol phosphates in bovine parathyroid cells. FEBS Lett. Jun 22 1987;218(1):113-8. Epub 1987/06/22.
25. Shoback DM, Membreno LA, McGhee JG. High calcium and other divalent cations increase inositol trisphosphate in bovine parathyroid cells. Endocrinology. Jul 1988;123(1):382-9. Epub 1988/07/01.
26. Chang W, Chen TH, Pratt S, Shoback D. Amino acids in the second and third intracellular loops of the parathyroid Ca2+-sensing receptor mediate efficient coupling to phospholipase C. The Journal of biological chemistry. Jun 30 2000;275(26):19955-63. Epub 2000/04/15.
27. Chakravarti B, Chattopadhyay N, Brown EM. Signaling through the extracellular calcium-sensing receptor (CaSR). Advances in experimental medicine and biology. 2012;740:103-42.
28. Kifor O, Diaz R, Butters R, Brown EM. The Ca2+-sensing receptor (CaR) activates phospholipases C, A2, and D in bovine parathyroid and CaR-transfected, human embryonic kidney (HEK293) cells. Journal of bone and mineral research : the official journal of the American Society for Bone and Mineral Research. May 1997;12(5):715-25. Epub 1997/05/01.

29. Wall MA, Coleman DE, Lee E, Iniguez-Lluhi JA, Posner BA, Gilman AG, et al. The structure of the G protein heterotrimer Gi alpha 1 beta 1 gamma 2. Cell. Dec 15 1995;83(6):1047-58.
30. Oldham WM, Hamm HE. Heterotrimeric G protein activation by G-protein-coupled receptors. Nature reviews Molecular cell biology. Review Jan 2008;9(1):60-71. Epub 2007/11/29.
31. Johnston CA, Siderovski DP. Receptor-mediated activation of heterotrimeric G-proteins: current structural insights. Molecular pharmacology. Aug 2007;72(2):219-30.
32. Kifor O, MacLeod RJ, Diaz R, Bai M, Yamaguchi T, Yao T, et al. Regulation of MAP kinase by calcium-sensing receptor in bovine parathyroid and CaR-transfected HEK293 cells. American journal of physiology Renal physiology. Feb 2001;280(2):F291-302.
33. Masuho I, Ostrovskaya O, Kramer GM, Jones CD, Xie K, Martemyanov KA. Distinct profiles of functional discrimination among G proteins determine the actions of G protein-coupled receptors. Science signaling. Dec 01 2015;8(405):ra123.
34. Leach K, Sexton PM, Christopoulos A, Conigrave AD. Engendering biased signalling from the calcium-sensing receptor for the pharmacotherapy of diverse disorders. British journal of pharmacology. Mar 2014;171(5):1142-55.
35. Holstein DM, Berg KA, Leeb-Lundberg LM, Olson MS, Saunders C. Calcium-sensing receptor-mediated ERK1/2 activation requires Galphai2 coupling and dynamin-independent receptor internalization. The Journal of biological chemistry. Mar 12 2004;279(11):10060-9.
36. Wettschureck N, Offermanns S. Mammalian G proteins and their cell type specific functions. Physiological reviews. Oct 2005;85(4):1159-204.
37. Van Raamsdonk CD, Griewank KG, Crosby MB, Garrido MC, Vemula S, Wiesner T, et al. Mutations in GNA11 in uveal melanoma. The New England journal of medicine. Dec 02 2010;363(23):2191-9.
38. Shi G, Partida-Sanchez S, Misra RS, Tighe M, Borchers MT, Lee JJ, et al. Identification of an alternative G{alpha}q-dependent chemokine receptor signal transduction pathway in dendritic cells and granulocytes. The Journal of experimental medicine. Oct 29 2007;204(11):2705-18.
39. Block GA, Martin KJ, de Francisco AL, Turner SA, Avram MM, Suranyi MG, et al. Cinacalcet for secondary hyperparathyroidism in patients receiving hemodialysis. The New England journal of medicine. Apr 08 2004;350(15):1516-25.

Figure Legends

Figure 1. Identification and structural assessment of a Phe220Ser $G\alpha_{11}$ mutation in a family with familial hypocalciuric hypercalcemia type 2. (**A**) The family comprised of 5 affected and 3 unaffected members (Top). The proband (individual II.1) is indicated by an arrow. A heterozygous T-to-C transition at nucleotide c.659, predicted to result in a missense substitution of the wild-type (WT) Phe to a mutant (m) Ser at codon 220 of the $G\alpha_{11}$ protein, was identified in the proband and confirmed to cosegregate with hypercalcemia by Sanger DNA sequence analysis. (**B**) Multiple protein sequence alignment of residues comprising the β3-α2 loop, α2-helix and α2-β4 loop that form switch II (red box) of $G\alpha_{11}$ orthologs (top) and Gα-subunit paralogs (bottom). Conserved residues are shown in gray, and WT (Phe, F) and mutant (Ser, S) residues are shown in red. (**C**) Structural model showing that Phe220 of $G\alpha_{11}$ is part of a hydrophobic cluster of amino acids (yellow) within switch II and the α3-helix, which stabilize the region in a conformation that facilitates effector binding. (**D**) Close-up view of Phe220 residue, within the switch II region of the GTPase domain of $G\alpha_{11}$, in complex with phospholipase C-β3 (brown space-filling model), with directly interacting residues of the α2 and α3 helices colored blue.

Figure 2. Effect of the mutant Ser220 $G\alpha_{11}$ on $Ca^{2+}{}_i$ and ERK signalling in HEK-CaSR cells. (**A**) $Ca^{2+}{}_i$ responses to changes in $[Ca^{2+}]_e$ of HEK-CaSR cells expressing WT (Phe220) or mutant (Ser220) $G\alpha_{11}$ proteins shown as the mean±SEM of 4-11 transfections. The Ser220 $G\alpha_{11}$ mutant caused a rightward shift in the $Ca^{2+}{}_i$ concentration-response curve with significantly increased EC_{50} value compared to WT cells (***$p<0.0001$, *F*-test). (**B**) $[Ca^{2+}]_e$-induced NFAT reporter responses, which are activated by elevations of $Ca^{2+}{}_i$, were assessed in HEK-CaSR cells expressing WT or mutant $G\alpha_{11}$ proteins. Responses at each $[Ca^{2+}]_e$ are

expressed as a fold-change of basal $[Ca^{2+}]_e$ responses, and shown as mean±SEM of 12 transfections. NFAT luciferase reporter activity increased in all cells in a concentration-dependent manner, and was significantly reduced in Ser220 cells compared to WT cells. (**C**) Ca^{2+}_e-induced pERK responses of cells expressing WT or mutant $G\alpha_{11}$ protein, expressed as a ratio to total ERK levels, and shown as mean±SEM of 8 transfections. (**D**) Ca^{2+}_e-induced SRE reporter responses of cells expressing WT or mutant $G\alpha_{11}$ protein, expressed compared to basal SRE reporter activity, and shown as mean±SEM of 8 transfections. The Ser220 $G\alpha_{11}$ mutant was associated with significantly decreased pERK and SRE reporter responses compared to WT. **p<0.01 and ****p<0.0001, by a 2-way ANOVA with Tukey's multiple-comparisons test.

Figure 3. Effect of $G\alpha_{11}$ residue 220 hydrophobicity on PLC-mediated signalling. (**A**) Histograms showing Ca^{2+}_e-induced Ca^{2+}_i EC_{50} values with 95% confidence intervals (CI) for cells expressing WT Phe220 or residue 220 mutant (m) $G\alpha_{11}$ proteins from 6-12 transfections. Statistical analyses were performed using the *F*-test. The Arg220 $G\alpha_{11}$ mutant reduced the EC_{50} value, whereas the Glu220 and Ser220 $G\alpha_{11}$ mutants elevated the EC_{50} value. (**B**) Ca^{2+}_e-induced NFAT reporter responses, which assess Ca^{2+}_i signaling, of cells expressing WT or residue 220 mutant $G\alpha_{11}$ proteins. Responses at each $[Ca^{2+}]_e$ are expressed as a fold-change of basal $[Ca^{2+}]_e$ responses, and shown as mean±SEM of 4-12 transfections. NFAT luciferase reporter activity increased in all cells in a concentration-dependent manner, however responses were significantly elevated in Arg220 $G\alpha_{11}$ mutant, and reduced in Glu220 $G\alpha_{11}$ mutant cells, compared to WT cells. (**C**) Ca^{2+}_e-induced pERK responses of cells expressing WT or mutant residue 220 $G\alpha_{11}$ proteins, expressed as a ratio to total ERK levels. The Arg220 mutant was associated with significantly increased responses, and the Glu220 and Ser220 mutants were associated with decreased responses, when compared to WT. Data are shown as mean±SEM

of 4-8 independent transfections. (**D**) Ca^{2+}_e-induced SRE reporter responses of cells expressing WT or mutant (m) residue 220 $G\alpha_{11}$ proteins, expressed as a ratio to total ERK levels. The engineered Arg220 mutant was associated with significantly increased, and the engineered Glu220 and FHH2-associated Ser220 mutants resulted in decreased responses, when compared to WT. Data are shown as mean±SEM of 4-8 independent transfections. Statistical analyses performed using 2-way ANOVA with Tukey's multiple-comparisons test comparing WT with $G\alpha_{11}$ mutants Ala220, Arg220, Glu220, and Ser220. *p<0.05, **p<0.01, ***p<0.001 ****p<0.0001.

Figure 4. Effect of mutating residues within the $G\alpha_{11}$ switch II-α3 hydrophobic cluster on PLC-mediated signalling. (**A**) Histograms showing Ca^{2+}_e-induced Ca^{2+}_i EC_{50} values with 95% CI for cells expressing WT and alanine (Ala) $G\alpha_{11}$ mutants (m) of residues 217, 223 and 263 $G\alpha_{11}$ proteins from 4-8 independent transfections. Only the Ala217 $G\alpha_{11}$ mutant increased the EC_{50} value, when compared to WT cells. Statistical analyses were performed using the *F*-test. (**B-C**) Ca^{2+}_e-induced (B) NFAT and (C) SRE luciferase reporter responses of cells expressing WT or alanine (Ala) $G\alpha_{11}$ mutants. Responses at each $[Ca^{2+}]_e$ are expressed as a fold-change of basal $[Ca^{2+}]_e$ responses, and shown as mean±SEM of 4-8 transfections. NFAT and SRE reporter responses were significantly reduced in Ala217 expressing cells compared to WT cells. (**D**) Histograms showing Ca^{2+}_e-induced Ca^{2+}_i EC_{50} values with 95% CI for cells expressing WT and glutamic acid (Glu) $G\alpha_{11}$ mutants (m) of residues 217, 223 and 263 from 4-8 independent transfections. All Glu $G\alpha_{11}$ mutants increased the EC_{50} value, when compared to WT cells. Statistical analyses were performed using the *F*-test. (**E-F**) Ca^{2+}_e-induced (E) NFAT and (F) SRE luciferase reporter responses of cells expressing WT or glutamic acid (Glu) $G\alpha_{11}$ mutants. Responses at each $[Ca^{2+}]_e$ are expressed as a fold-change of basal $[Ca^{2+}]_e$ responses, and shown as mean±SEM of 4-8 transfections. NFAT and SRE reporter responses were significantly

reduced in cells expressing all 3 glutamic acid mutants compared to WT cells. Statistical analyses for panels B, C, E and F were performed using 2-way ANOVA with Tukey's multiple-comparisons test comparing WT to mutant 217 (green), 223 (red) and 263 (gray) $G\alpha_{11}$ proteins. *p<0.05, ***p<0.001, ****p<0.0001.

Figure 5. Effect of cinacalcet on the loss-of-function and hypercalcemia caused by the Phe220Ser $G\alpha_{11}$ mutation. (**A**) Effect of cinacalcet on $Ca^{2+}{}_i$ responses to changes in $[Ca^{2+}]_e$ of HEK-CaSR cells transfected with WT or Ser220 $G\alpha_{11}$ mutant (m). The $Ca^{2+}{}_i$ responses to changes in $[Ca^{2+}]_e$ are expressed as a percentage of the maximum normalized responses and shown as the mean±SEM of 6-12 independent transfections. The Ser220 $G\alpha_{11}$ mutant led to a rightward shift in the concentration-response curve. The addition of 30 nM cinacalcet, a concentration previously shown to rectify the loss-of-function associated with the reported Leu135Gln $G\alpha_{11}$ FHH2 mutant *in vitro* [10], had no effect on Ser220 responses. However, addition of 100 nM cinacalcet rectified the rightward shift of the Ser220 $G\alpha_{11}$ mutant, such that it was not different to WT responses. (**B-C**) Histograms showing (**B**) NFAT and (**C**) SRE luciferase reporter activity in response to 5mM $Ca^{2+}{}_e$ in HEK-CaSR cells expressing WT or Ser220 mutant constructs, treated with vehicle or cinacalcet (CIN). Data are shown as mean±SEM of 4 independent transfections. 100 nM cinacalcet was required to significantly increase NFAT and SRE reporter activity to WT levels. The responses of cells expressing WT or mutant $G\alpha_{11}$ proteins were compared using the *F*-test for panel A and 2-way ANOVA with Tukey's multiple-comparisons test for panel B and C. **p<0.01, ***p<0.001, ****p<0.0001. (**D**) Effect of cinacalcet on the serum ionized calcium concentrations of the FHH2 proband (individual II.1, Figure 1A) with the Phe220Ser $G\alpha_{11}$ mutation. Arrows indicate initiation of oral cinacalcet at 30 mg/day (CIN 30), at 60 mg/day (CIN 60), and its discontinuation. Cinacalcet treatment decreased serum concentrations of ionized calcium and PTH from 98 ng/L (pre-treatment) to 58 ng/L (post-treatment) (normal range 8-73 ng/L). Shaded area indicates normal range.

Table 1. Clinical and biochemical findings in available affected members of the family with the Phe220Ser Gα11 mutation.

Variable	Individual			
	II.1	III.2	III.3	III.4
Sex	Male	Female	Male	Female
Age at diagnosis	33 years	7 weeks	At birth	18 months
Associated clinical features	Headaches, pruritus, constipation[a]	Constipation, scoliosis, headaches[b]	Premature birth[c], eczema, constipation	Constipation, eczema
Serum biochemistry[d]:				
Ionized calcium (mmol/L)	1.42	1.41	1.46	1.46
Phosphate (mmol/L)	0.50	1.98	1.81	1.62
Alkaline phosphatase (U/L)	77	275	461	243
Magnesium (mmol/L)	0.78	1.00	0.90	0.93
Creatinine (µmol/L)	76	26	78	26
PTH (ng/L)	98	39	100	40
25-hydroxyvitamin D (nmol/L)	49	50	102	122
Thyrotropin (mU/L)	2.82	1.83	5.5[e]	1.53
Urinary calcium excretion	0.09	0.002	0.001	0.003

[a]A skin biopsy demonstrated folliculitis with keratin within the widened hair follicle and inflammatory cells around the hair follicle. Normal bone mineral density T-score ≥-1.0 at lumbar spine and femoral neck. [b]Individual III.2 (Figure 1) developed headaches from age 10 years. [c]Individual III.3 was born prematurely at gestational age 27+3 weeks. [d]Normal biochemical ranges: ionized calcium, 1.16-1.30 mmol/L (adults) and 1.16-1.39 mmol/L (age 1-12 months); phosphate, 1.50-2.60 mmol/L (neonates), 1.50-2.50 mmol/L (age 1-6 months), 1.20-1.80 mmol/L (age 2-12 years) and 0.71-1.53 mmol/L (adults); alkaline phosphatase activity, 35-105 U/L (adults) and 115-460 U/L (age 15 days-1 year); magnesium, 0.71-0.94 mmol/L (adults) and 0.7-1.0 mmol/L (age 3 months-17 years); creatinine, 60-100 µmol/L (adult males) and 10-56 µmol/L (age 8 days-2 years); PTH, 8-73 ng/L; 25-hydroxyvitamin D, >50 nmol/L; thyrotropin; 0.5-3.6 mU/L (age >14 weeks) and 0.4-7 mU/L (age 11-14 weeks); calcium-to-creatinine clearance ratio >0.02. [e]TSH concentration measured in umbilical cord blood (normal range not available for premature infant cord blood TSH).

Figure 1

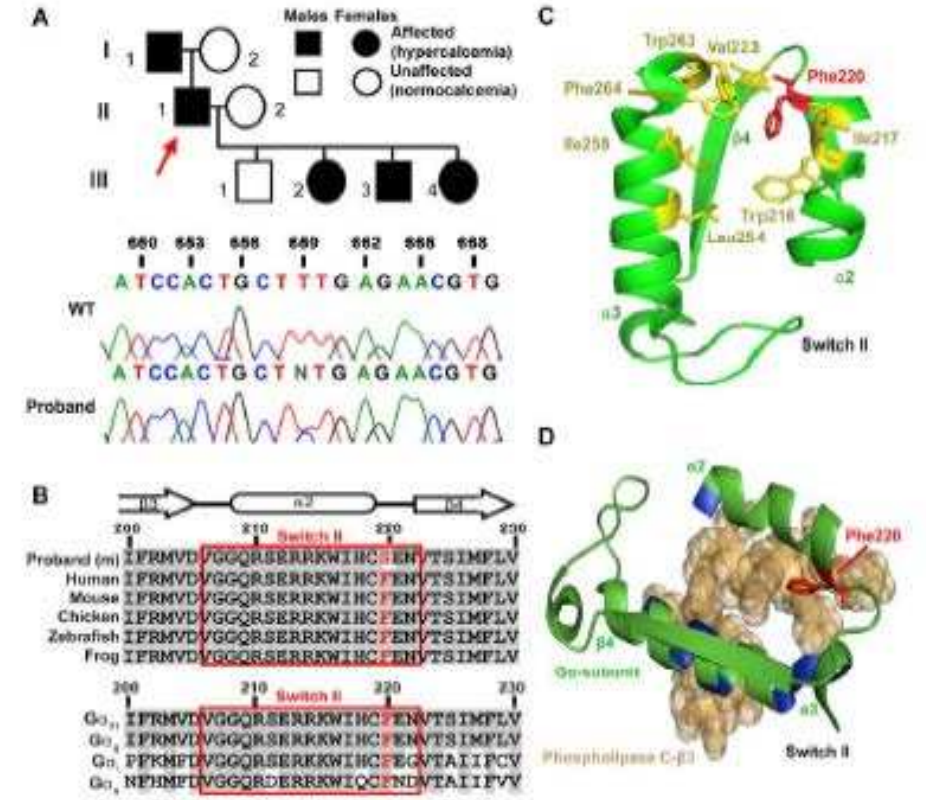

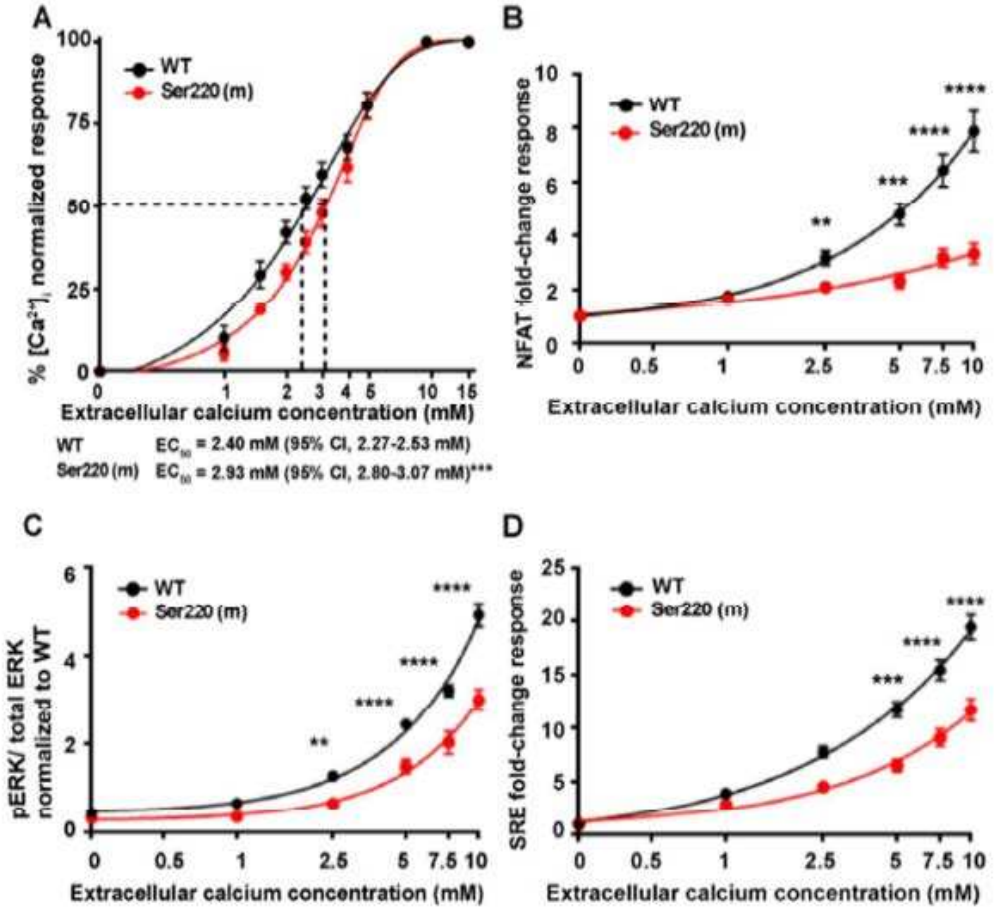

Figure 2

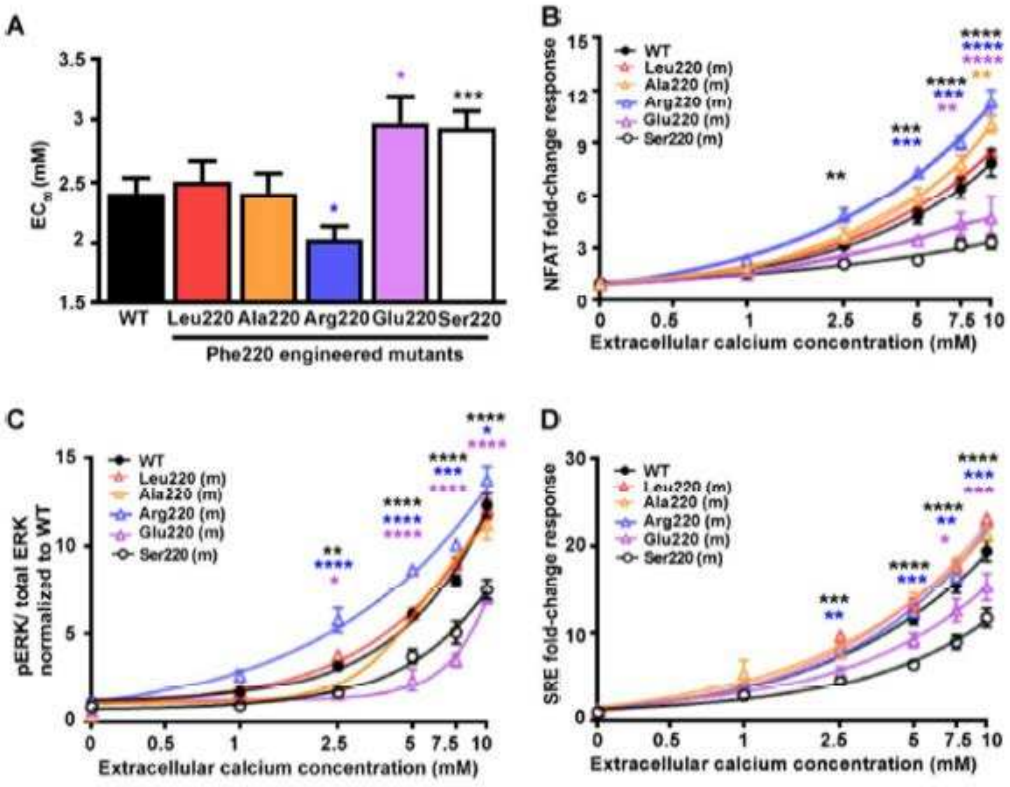

Figure 3

Figure 4

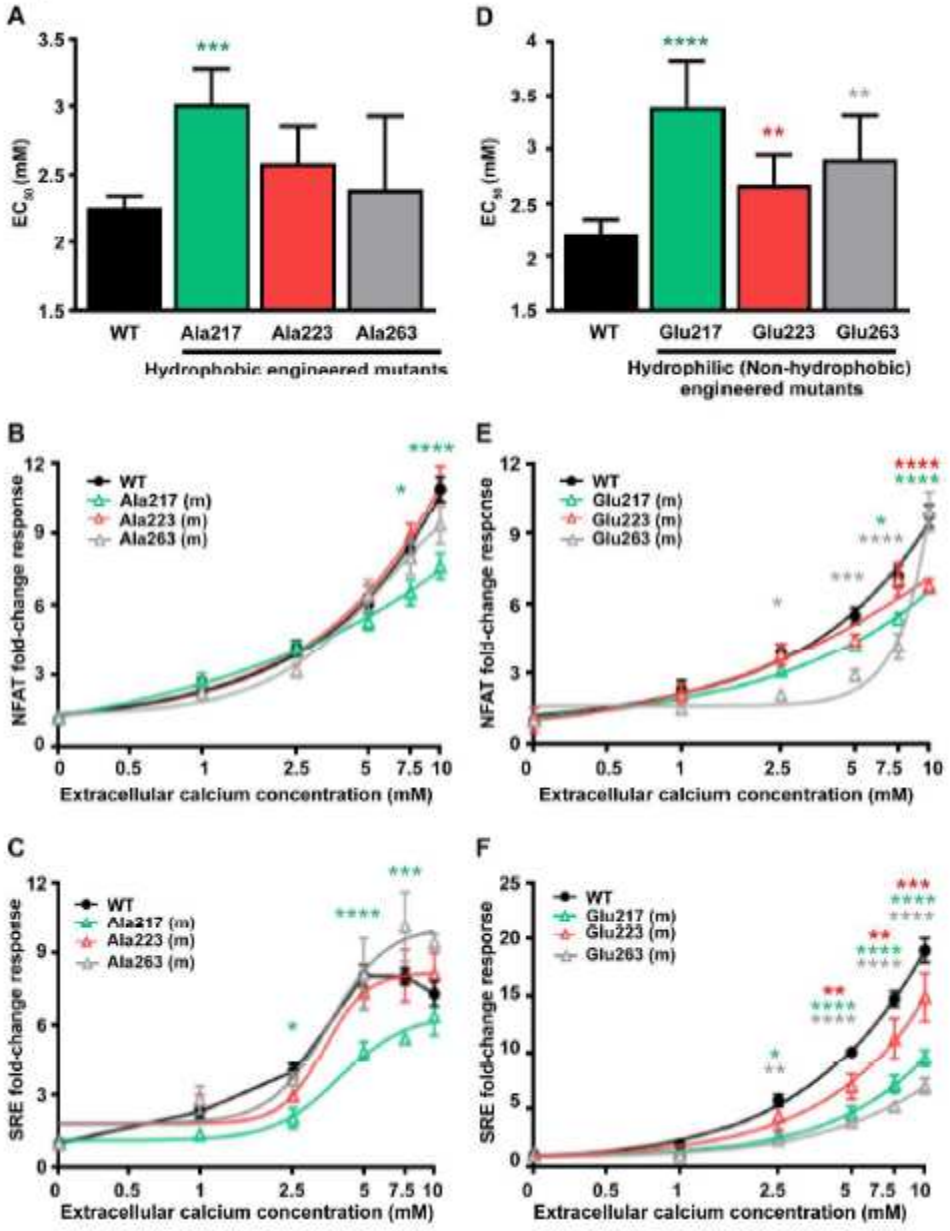

Figure 5